

# Electronic Supplementary Information

## Cost-Effective Synthesis of Furan- and Thienyl-Based Microporous Polyaminals for Adsorptions of Gases and Organic Vapors

Guiyang Li,<sup>a,b</sup> Biao Zhang,<sup>a</sup> Jun Yan<sup>a</sup> and Zhonggang Wang<sup>\*a</sup>

<sup>a</sup> State Key Laboratory of Fine Chemicals, Department of Polymer Science and Materials, School of Chemical Engineering, Dalian University of Technology, Dalian 116024, China

<sup>b</sup> Aerospace Research Institute of Materials & Processing Technology, Beijing, 100076, China

Email: zgwang@dlut.edu.cn

### Contents

**Table S1** Porosity Parameters of PAN-F and PAN-T Obtained by N<sub>2</sub> Adsorption at 77 K.

**Table S2** Uptakes of H<sub>2</sub>, CO<sub>2</sub> and selectivity of CO<sub>2</sub>/N<sub>2</sub> for PAN-F and PAN-T.

**Table S3**  $K_H$ ,  $A_o$ ,  $A_1$  and  $Q_o$  values of CO<sub>2</sub> adsorption for PAN-F and PAN-T.

**Table S4**  $K_H$ ,  $A_o$ ,  $A_1$  and  $Q_o$  values of H<sub>2</sub> adsorption for PAN-F and PAN-T.

**Table S5** Uptakes of organic vapors for PAN-F and PAN-T.

**Fig. S1** FTIR spectra of PAN-F and PAN-T.

**Fig. S2** Solid-state <sup>13</sup>C CP/MAS NMR spectra for PAN-F and PAN-T.

**Fig. S3** Solid-state <sup>13</sup>C MAS NMR spectrum for PAN-T.

**Fig. S4** FE-SEM images of PAN-F and PAN-T.

**Fig. S5** Wide angle X-ray diffractions of PAN-F and PAN-T.

**Fig. S6** Experimental pure component adsorption isotherms for CO<sub>2</sub> and N<sub>2</sub> at 273 K, and the corresponding single-site Langmuir-Freundlich fitting curves for PAN-F and PAN-T.

**Fig. S7** Adsorption selectivity of CO<sub>2</sub> over N<sub>2</sub> for PAN-F and PAN-T from initial slope calculations of CO<sub>2</sub> and N<sub>2</sub> isotherms at 273 K.

**Fig. S8** IAST selectivity for 0.15/0.85 CO<sub>2</sub>/N<sub>2</sub> mixture as a function of pressure for PAN-F and PAN-T.

**Fig. S9** Virial plots of H<sub>2</sub> adsorption in PAN-F and PAN-T at 77 and 87 K.

### Experimental Section

**Table S1** Porosity parameters of PAN-F and PAN-T obtained by N<sub>2</sub> adsorption at 77 K.

Sample	$S_{\text{BET}}$ (m <sup>2</sup> g <sup>-1</sup> )	$S_{\text{Langmuir}}$ (m <sup>2</sup> g <sup>-1</sup> )	$S_{\text{micro}}$ (m <sup>2</sup> g <sup>-1</sup> )	$V_{\text{micro}}$ (m <sup>3</sup> g <sup>-1</sup> )	$V_{\text{total}}$ (cm <sup>3</sup> g <sup>-1</sup> )	Pore size (nm)
PAN-F	702	1095	147	0.07	0.89	0.68
PAN-T	795	1167	365	0.17	0.73	0.59

**Table S2** Uptakes of H<sub>2</sub>, CO<sub>2</sub>, and CO<sub>2</sub>/N<sub>2</sub> selectivity for PAN-F and PAN-T.

Sample	H <sub>2</sub> uptake (wt%) <sup>a</sup>		CO <sub>2</sub> uptake (wt%) <sup>b</sup>		CO <sub>2</sub> /N <sub>2</sub> selectivity <sup>c</sup>	
	77 K	87 K	273 K	298 K	Henry law	IAST
PAN-F	0.85	0.69	10.0	7.5	36.0	42.8
PAN-T	1.27	0.82	14.8	11.5	45.8	68.4

<sup>a</sup>) Uptakes for H<sub>2</sub> determined at 1 bar. <sup>b</sup>) Uptakes for CO<sub>2</sub> determined at 1 bar. <sup>c</sup>) Henry law selectivity of CO<sub>2</sub>/N<sub>2</sub> was calculated from the ratio of initial slope of CO<sub>2</sub> to N<sub>2</sub> in the pure-component adsorption isotherms at 273 K, whereas IAST selectivity of CO<sub>2</sub>/N<sub>2</sub> was calculated from 0.15/0.85 gas mixture for CO<sub>2</sub>/N<sub>2</sub> at 273 K and 1 bar.

**Table S3**  $K_H$ ,  $A_o$ ,  $A_I$  and  $Q_o$  values of CO<sub>2</sub> adsorption in PAN-F and PAN-T.

Samples	$T$ K	$K_H$ mol g <sup>-1</sup> Pa <sup>-1</sup>	$A_o$ ln(mol g <sup>-1</sup> Pa <sup>-1</sup> )	$A_I$ g mol <sup>-1</sup>	$Q_o$ kJ mol <sup>-1</sup>
PAN-F	273	$1.749 \times 10^{-7}$	-15.559	-1291.684	31.7
	298	$5.418 \times 10^{-8}$	-16.731	-986.977	
PAN-T	273	$3.692 \times 10^{-7}$	-14.812	-1130.751	36.3
	298	$9.618 \times 10^{-8}$	-16.157	-781.632	

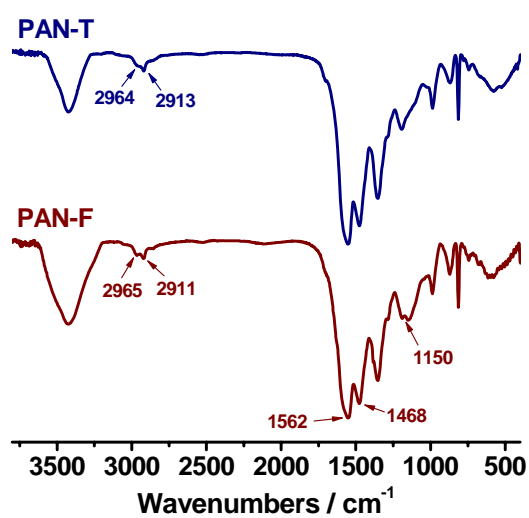
**Table S4**  $K_H$ ,  $A_o$ ,  $A_I$  and  $Q_o$  values of  $H_2$  adsorption in PAN-F and PAN-T.

Samples	$T$ K	$K_H$ $\text{mol g}^{-1} \text{Pa}^{-1}$	$A_o$ $\ln(\text{mol g}^{-1} \text{Pa}^{-1})$	$A_I$ $\text{g mol}^{-1}$	$Q_o$ $\text{kJ mol}^{-1}$
PAN-F	77	$2.521 \times 10^{-6}$	-12.891	-1178.218	6.79
	87	$7.434 \times 10^{-7}$	-14.112	-1361.510	
PAN-T	77	$4.082 \times 10^{-6}$	-12.409	-942.402	7.41
	87	$1.081 \times 10^{-6}$	-13.737	-1039.750	

**Table S5** Uptakes of organic vapors for PAN-F and PAN-T.

Sample	Vapor uptake (wt%, 298 K) <sup>a</sup>		
	$C_6H_6$	$c-C_6H_{12}$	$H_2O$
PAN-F	54.4	43.3	12.8
PAN-T	57.0	51.8	16.2

<sup>a</sup>) Uptakes for  $C_6H_6$  (benzene vapor),  $c-C_6H_{12}$  (cyclohexane vapor) and  $H_2O$  (water vapor) were determined at  $P/P_0 = 0.9$ .

**Fig. S1** FTIR spectra of PAN-F and PAN-T.

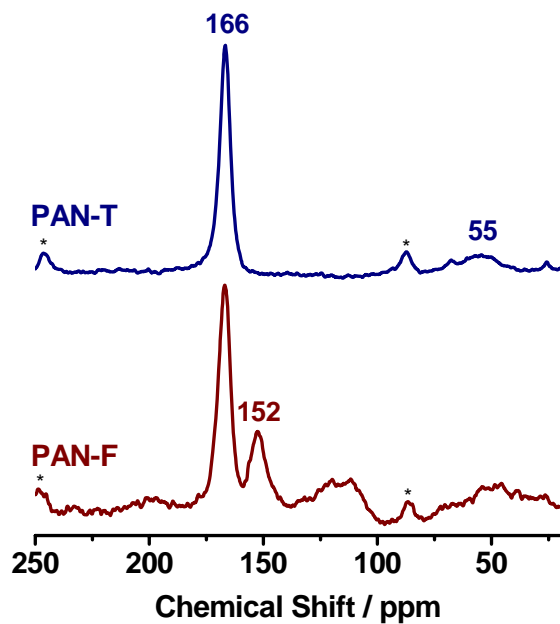


**Fig. S2** Solid-state  $^{13}\text{C}$  CP/MAS NMR spectra for PAN-F and PAN-T. Asterisks (\*) indicate peaks arising from spinning side bands.

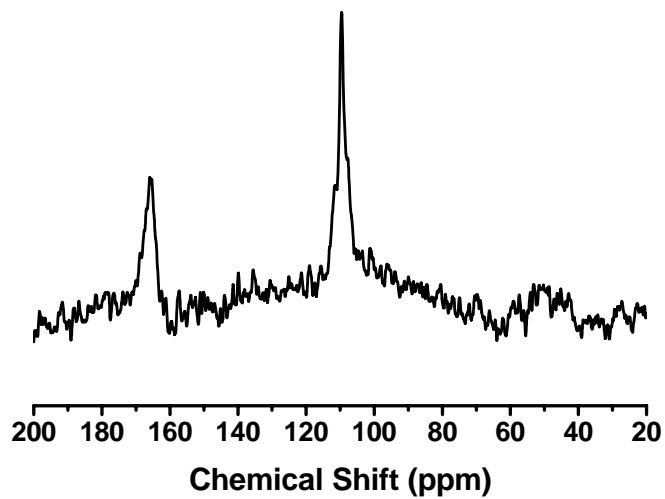


**Fig. S3** Solid-state  $^{13}\text{C}$  MAS NMR spectrum for PAN-T.

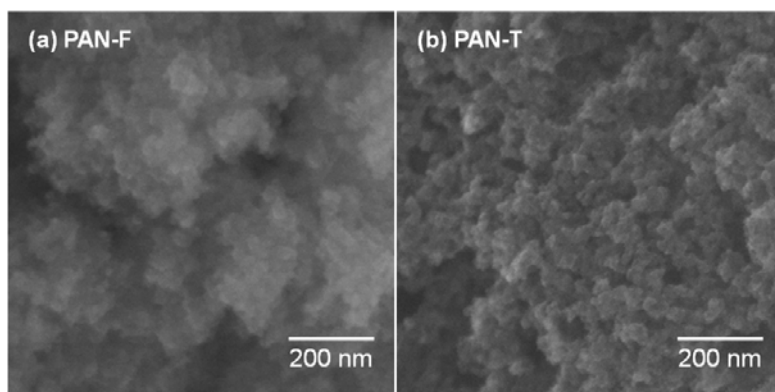


**Fig. S4** Field-emission SEM images of PAN-F and PAN-T.

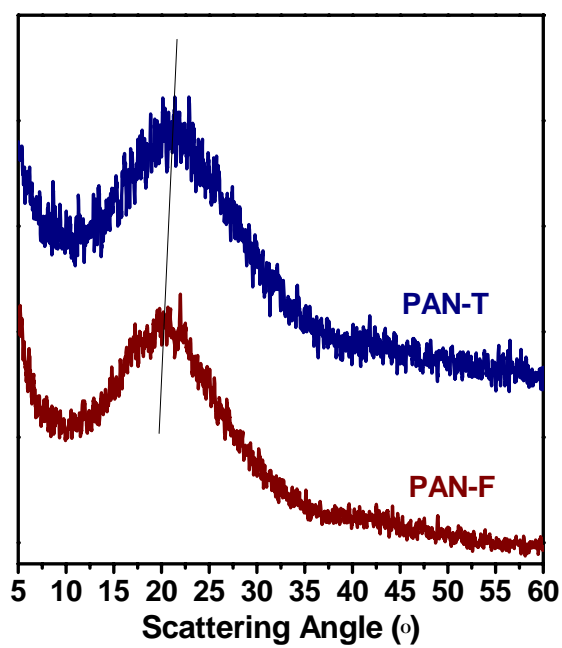


**Fig. S5** Wide angle X-ray diffractions of PAN-F and PAN-T.

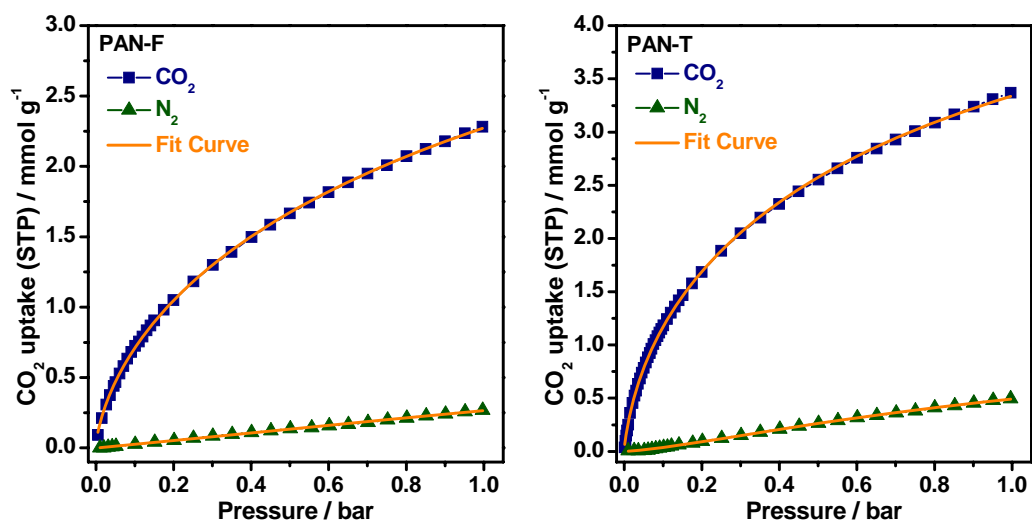


**Fig. S6** Experimental pure component adsorption isotherms for CO<sub>2</sub> and N<sub>2</sub> at 273 K, and the corresponding single-site Langmuir-Freundlich fitting curves for PAN-F and PAN-T.

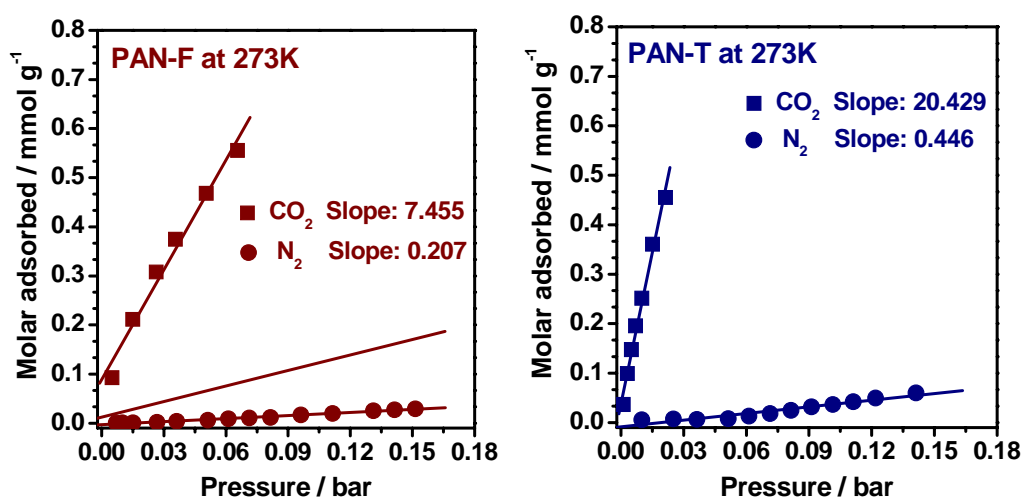


**Fig. S7** Adsorption selectivity of CO<sub>2</sub> over N<sub>2</sub> for PAN-F and PAN-T from initial slope calculations of CO<sub>2</sub> and N<sub>2</sub> isotherms at 273 K.

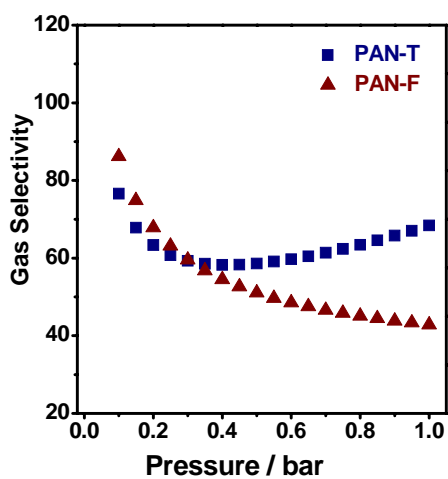


**Fig. S8** IAST selectivity for 0.15/0.85 CO<sub>2</sub>/N<sub>2</sub> mixture as a function of pressure for PAN-F and PAN-T.

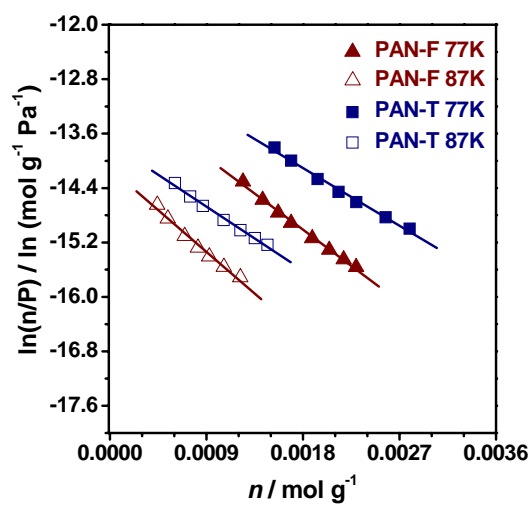


**Fig. S9** Virial plots of H<sub>2</sub> adsorption in PAN-F and PAN-T at 77 and 87 K.

## Experimental Section

**Materials.** Melamine, 2-furaldehyde and 2-thenaldehyde were purchased from J&K Chemical Co., Ltd. Dimethyl sulfoxide (DMSO), tetrahydrofuran (THF), *N,N*-dimethylformamide (DMF) and other reagents were purchased from Shanghai Chemical Reagent Co. DMSO was purified by distillation under reduced pressure and dehydrated with 4Å molecular sieves, and other reagents were of reagent grade and used as received.

**Instrumentation.** Fourier transform infrared spectra (FTIR) of synthesized products were recorded using a Nicolet 20XB FT-IR spectrophotometer in 400–4000  $\text{cm}^{-1}$ . Samples were prepared by dispersing the complexes in KBr to form disks. Solid-state  $^{13}\text{C}$  CP/MAS (cross-polarization with magic angle spinning) spectra were measured on a Varian Infinity-Plus 400 spectrometer at 100.61 MHz at an MAS rate of 10.0 kHz using zirconia rotors 4 mm in diameter using a contact time of 4.0 ms and a relaxation delay of 2.0 s. Wide-angle X-ray diffractions (WAXD) from  $5^\circ$  to  $60^\circ$  were performed on Rigku D/max-2400 X-ray diffractometer (40 kV, 200 mA) with a copper target at a scanning rate of  $2^\circ/\text{min}$ . Field-emission scanning electron microscopy (FE-SEM) experiments were carried on a Nova NanoSEM 450. Adsorption and desorption measurements for all the gases and vapors were conducted on an Autosorb iQ (Quantachrome) analyzer. Prior to measurements, the samples were degassed at  $120^\circ\text{C}$  under high vacuum overnight.

**Preparation of microporous polyaminal networks (PAN-F and PAN-T).** The polymerizations of PAN-F and PAN-T were carried out in a similar procedure. Only the



polymerization of PAN-T is described here as an example. A dry Schlenk flask equipped with a stirrer and a condenser was degassed using two evacuation-argon-backfill cycles. Under argon flow, melamine (0.50 g, 3.96 mmol), 2-thenaldehyde (0.80 g, 7.16 mmol) and 25 mL DMSO were added and heated at 180 °C for 72 h. Finally, the system was cooled down and the solid was isolated, washed successively with DMF, methanol and THF. The resultant product was extracted with THF in a Soxhlet apparatus for 24 h, and dried at 120 °C under vacuum to constant weight with a quantitative yield.

The enthalpy of adsorption at zero coverage ( $Q_0$ ) can be investigated from the CO<sub>2</sub> isotherms at different temperatures using virial equation:

$$\ln(n/P) = A_0 + A_1 \cdot n + A_2 \cdot n^2 + \dots \quad (1)$$

where  $n$  is the adsorbed amount at pressure  $P$ , and  $A_0$ ,  $A_1$ , etc. are virial coefficients. At low surface coverage,  $A_2$  and higher terms can be neglected, thus, the Henry's law constant ( $K_H$ ) can be calculated by equation of  $K_H = \exp(A_0)$ . Based on the  $K_H$  values at different temperature, the  $Q_0$  value is derived from the slope of the plot of  $\ln K_H$  versus  $1/T$ .

Ideal adsorbed solution theory (IAST) was performed to evaluate the adsorption selectivities of CO<sub>2</sub>/CH<sub>4</sub> and CO<sub>2</sub>/N<sub>2</sub> gas mixtures.<sup>1</sup> According to Myers and Prausnitz, the method of IAST can be reduced to the mathematical integration:

$$\int_{x_1}^{Py_1} F_1(t) d \ln t = \int_{x_2}^{Py_2} F_2(t) d \ln t \quad (2)$$

where  $P$  is the total pressure,  $x_i$  is the adsorbed phase molar ratio of gas  $i$ ,  $y_i$  is the bulk phase

molar ratio of gas  $i$  and the function  $F_i(t)$  is a fitting function for the pure component  $i$  based on the single-site or dual-site Langmuir-Freundlich model:

$$n = \frac{a \cdot b \cdot p^{1/c}}{1 + b \cdot p^{1/c}} \quad (3)$$

Where  $n$  is amount of gas adsorbed ( $\text{mmol g}^{-1}$ ),  $p$  is the pressure (bar) of the bulk gas at equilibrium with the adsorbed phase,  $a$  is the saturation capacity ( $\text{mmol g}^{-1}$ ),  $b$  is the single-site affinity coefficient ( $1/\text{bar}$ ),  $c$  is the deviation from an ideal homogeneous surface. These isothermal parameters ( $a$ ,  $b$ ,  $c$ ) are the fitting parameters according to the experimental pure-component isotherms of  $\text{N}_2$ ,  $\text{CO}_2$  and  $\text{CH}_4$ .

Since  $x_1 + x_2 = 1$  and  $y_1 + y_2 = 1$ , the adsorption selectivity ( $\alpha_{A/B}$ ) of gas A over gas B is defined as:

$$\alpha_{A/B} = \frac{x_A / y_A}{x_B / y_B} \quad (4)$$